SAN FRANCISCO ESTUARY & WATERSHED SCIENCE
Sponsored by the Delta Stewardship Council and UC Davis Institute of the Environment

RESEARCH

A Simplified Approach for Estimating Ionic Concentrations from Specific Conductance Data in the San Francisco Estuary

Paul H. Hutton [1], Arushi Sinha [1], Sujoy B. Roy [1], and Richard A. Denton [2]

ABSTRACT

This work presents a simplified approach for estimating ionic concentrations from specific electrical conductance (EC) data in the San Francisco Estuary. Monitoring the EC of water through electrodes is simple and inexpensive. As a result, a wealth of high-resolution time-series data is available to indirectly estimate salinity concentrations and, by extension, seawater intrusion throughout the study domain. However, scientists and managers are also interested in quantifying ionic (e.g., bromide, chloride) and total dissolved solids (TDS) concentrations to meet water-quality regulations, protect beneficial uses, support environmental analyses, and track source-water dominance. These constituent concentrations, reported with lower spatial and temporal resolution than EC, are typically measured in the laboratory from discrete (grab) water samples. We divided the study domain into four unique regions to estimate concentrations of major ions and TDS as mathematical functions of measured or model-simulated EC. Salinity relationships in three of the four regions—regions that represent Sacramento–San Joaquin Delta (Delta) inflow and seawater-dominated boundaries—reflect ionic make-ups that are either independent of or weakly dependent on season and hydrologic condition, and are highly correlated with EC. The fourth region—represented by the interior Delta—exhibits salinity characteristics associated with complex-boundary source-water mixing that varies by season and hydrologic condition. We introduce a novel method to estimate ionic and dissolved solids concentrations within this fourth region, given month, water year type, and (optionally) X2 isohaline position, which allows for more accurate EC-based estimates than previously available. The resulting approach, while not a substitute for hydrodynamic modeling, can provide useful information under constrained schedules and budgets.

SFEWS Volume 21 | Issue 4 | Article 6

https://doi.org/10.15447/sfews.2023v21iss4art6

* Corresponding author email: sujoy.roy@tetratech.com

1 Tetra Tech, Inc.
Lafayette, CA 94549 USA

2 Richard Denton & Associates
Oakland, CA 94611 USA

KEY WORDS

major ion concentrations, regression, source water mixing, X2 isohaline, MWQI Program

INTRODUCTION

Salinity in California's San Francisco Estuary (estuary) is an important factor that affects the drinking water supply for 25 million residents, the ecosystem health of threatened and endangered fish species, and agricultural production. Salinity is highly managed through operation of upstream reservoirs and Sacramento–San Joaquin Delta (Delta) export pumps and flow control structures (Hutton et al. 2017) and is typically measured as specific electrical conductance (EC). Salinity monitoring through *in situ* electrodes is simple and inexpensive. As a result, a wealth of high-resolution time-series EC data is available to indirectly estimate salinity concentrations and, by extension, seawater intrusion throughout the study domain. However, scientists and managers are also interested in quantifying ionic (e.g., bromide, chloride) and total dissolved solids (TDS) concentrations to meet water-quality regulations, protect beneficial uses, support environmental analyses, and track source-water dominance. These constituent concentrations, reported with lower spatial and temporal resolution than EC, are typically measured in the laboratory from discrete (grab) water samples.

Salinity has been measured throughout the study domain since the early 20th century. In 1905, the US Geological Survey (USGS) established a sampling station above the City of Sacramento (see Figure 1) to characterize the mineralogy of freshwater inflows to the Delta from the Sacramento River (Van Winkle and Eaton 1910). The initial finding concluded that "… the water of the Sacramento River should be classed as carbonate—calcium, magnesium and bicarbonates forming the greater part of the dissolved mineral matter. The total dissolved solids are not high, and the water is fit for almost any industry that can use moderately hard water." A comprehensive investigation of salinity conditions in the study domain, focused on understanding salt intrusion from the upper estuary to the Delta, was first undertaken by the State of California's Water Supervisor in the summer of 1920, and continued for over 5 decades. Water samples were collected in support of this investigation at 4-day intervals about 1.5 hours after the predicted high tide, thereby allowing for an estimate of daily maximum salinity at each site. Salinity was measured through laboratory procedures and reported as chlorinity (parts of chlorine per 100,000 parts of water) (CDPW 1931; Hutton et al. 2015). In 1971, the Water Supervisor investigation was superseded by a compliance monitoring program outlined in the California State Water Resources Control Board's (CSWRCB) Water Rights Decision 1379 (CSWRCB 1971) that established a network of stations to measure continuous EC and discrete ionic constituents in the Delta and downstream of the Sacramento–San Joaquin River confluence. This compliance monitoring program continues and is managed by the Interagency Ecological Program to support the CSWRCB Water Rights Decision 1641 (Martinez and Perry 2021). The California Department of Water Resources (CDWR) complements compliance monitoring through its Municipal Water Quality Investigations (MWQI) Program, a program which has focused on municipal beneficial uses of Delta water since 1990. The MWQI Program measures an extensive suite of salinity constituents through continuous as well as discrete sampling—including EC, major anions (including bromide) and cations, and TDS—to assess source-water movement under various hydrologic conditions (Hutton et al. 2022a; Denton 2015).

Given the lower spatial and temporal resolution associated with measured ionic constituents, environmental analyses and associated salinity modeling are typically based on EC or EC-derived practical salinity (Lewis 1980; Schemel 2001; Hutton and Roy 2023a). However, water-quality regulations and beneficial-use targets are often based on more specific ionic measures. For example:

- A key water-quality regulation (CSWRCB 2000) governing the operation of Delta facilities by the California State Water Project (SWP) and federal Central Valley Project (CVP) is a chloride standard at the intake to the Contra Costa Canal at Rock Slough. These facilities (see Figure 1) are operated to maintain sufficient Delta outflow to ensure that chloride concentration at this location does not exceed

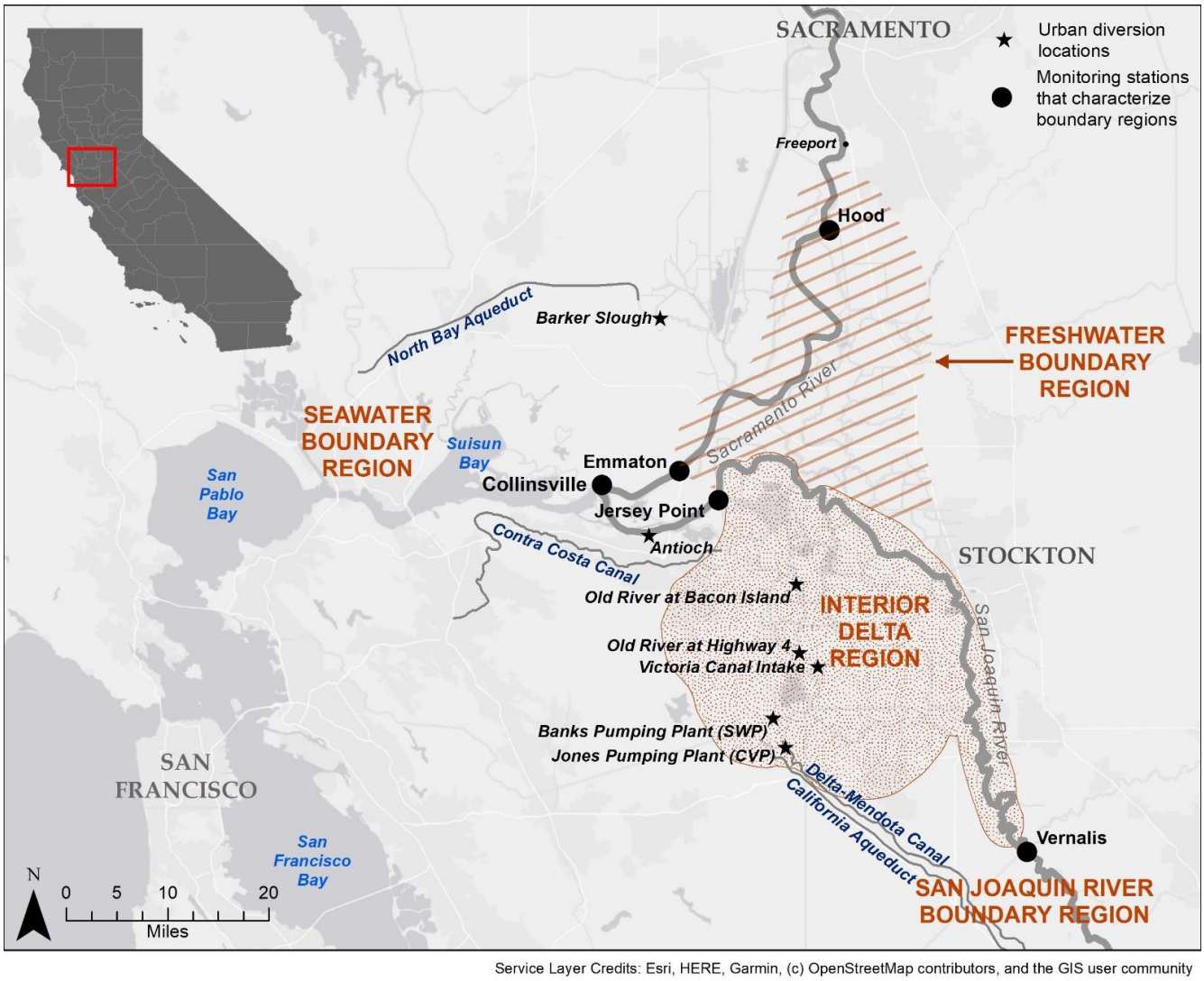

Figure 1 Delineation of boundary regions, the interior Delta region, and urban diversions

250 mg L^{-1} year-round, and that it does not exceed 150 mg L^{-1} at either this location or an alternate compliance location on the San Joaquin River at Antioch for more than 155 to 240 days per calendar year, depending upon water year type. Water years in California begin on October 1 of the preceding calendar year.

- Salinity intrusion introduces ocean-derived bromide salts to the interior Delta (Hutton and Chung 1992). This salinity ion is of special concern for municipal beneficial uses of Delta water, because it promotes the formation of several disinfection by-products that are suspected threats to human health when present in sufficient quantities in drinking water (Najm and Krasner 1995). Bromine-containing disinfection by-products are of greater health concern than their chlorine-containing analogs (Wagner and Plewa 2017).

- SWP contractors that serve municipalities have raised concerns about low alkalinity levels in exported Delta waters, prompting the MWQI Program to develop capabilities to simulate and forecast bicarbonate fate and transport in the Delta (Hutton et al. 2022a). Low alkalinity levels pose challenges to water treatment in the areas of coagulation and

https://doi.org/10.15447/sfews.2023v21iss4art6

corrosion control. Furthermore, alkalinity concentrations below 60 mg L^{-1} (as $CaCO_3$) are of concern to operators who treat Delta water, because greater total organic carbon removal is required under the US Environmental Protection Agency's Stage 1 Disinfection/ Disinfection Byproduct Rule (Fed Regist 1998). These concern levels are associated with periods of high winter and spring inflow to the Delta from the San Joaquin River that occur in wetter years.

- SWP contracts contain water-quality objectives for several salinity constituents, including TDS, total hardness, chloride, sulfate, and sodium. The state of California agreed to take all reasonable measures to make available SWP water to its contractors that does not exceed specific concentration limits for these constituents (for example, see CDWR 2003).

Thus, an ongoing need exists to estimate salinity constituent concentrations from available EC measurements and modeling data. Mathematical relationships between EC, TDS, and ionic concentrations can vary greatly by source water (Hem 1985; Denton 2015). For example, riverine inflows to the Delta have ionic make-ups that are approximately independent of season and hydrologic condition and are highly correlated with EC (Hutton et al. 2022b), while the ionic make-up of the western Delta and downstream estuary is weakly dependent on such conditions (Hutton and Roy 2023b). In contrast, a sizeable portion of the interior Delta exhibits salinity characteristics associated with complex mixing of different boundary sources of water that defy simple and direct mathematical relationships between EC and ionic concentrations.

The purpose of this work is to develop a simplified yet comprehensive approach to estimating ionic and dissolved solids concentrations throughout the estuary as a function of EC values; the approach is targeted toward a broad stakeholder community and does not require a specialized modeling background. Building upon recent work that focused on the study domain's seawater boundary region (Hutton and Roy 2023b), mathematical relationships are developed for the Delta inflow boundaries that are generally expressed as polynomial (quadratic) equations where constant terms are determined through ordinary least-squares regression of available grab sample data. We introduce a novel method to estimate ionic and dissolved solids concentrations within the interior Delta from a known EC value, given month, water year type, and (optionally) 2 parts-per-thousand (ppt) bottom salinity (X2) isohaline position (Hutton et al. 2015), which allows for more accurate EC-based estimates than previously available. The resulting approach, while not a substitute for hydrodynamic modeling, can provide useful information under constrained schedules and budgets. Additional details on this simplified approach are provided elsewhere (Hutton et al. 2022b).

BACKGROUND

In many respects, the concept of salinity in natural water bodies is quite simple. From a layperson's perspective, salinity is the "saltiness" or amount of salt dissolved in a given volume of water. But from a scientific perspective, salinity is associated with one or more specific measurement techniques. Here, we provide a brief background on how the concept or scientific definition of salinity has evolved over time. Following this historical survey, we describe the study setting and summarize previous work on estimating ionic concentrations from EC values for this domain.

Concept of Salinity

One of the most important and most frequently studied parameters of ocean and estuarine waters is its salt content or salinity. Unfortunately, no straightforward method is available to directly measure salinity, in part because of the number of dissolved solids found in these waters. The most obvious method—evaporating the water and weighing the residue—is problematic since various dissolved elements oxidize or vaporize at high temperatures (Hem 1985). Total dissolved solids (TDS), the term commonly applied to the weight of this residue, quantifies ionic components of salinity as well as other dissolved

inorganic and organic constituents that are not volatilized through the evaporation process. A complete chemical analysis of the dissolved constituents of salinity, while possible, is too time-consuming for routine use. Robert Boyle, considered by many experts to be the founder of the science now referred to as chemical oceanography (Wallace 1974), investigated ocean salinity in the 17th century by direct evaporation, and later measured density as an index of salinity.

The idea that sea water constituents exist in constant proportions became widely accepted in the scientific community in the 19th century (Culkin and Smed 1979). Using this concept—along with the fact that chloride could be determined accurately and precisely—Forchhammer, Knudsen, and other researchers developed a measure of salinity based on a "chlorinity" determination and a constant linear relationship between chlorinity and salinity (Wallace 1974). As noted in the Introduction, chlorinity was used as the measure of salinity intrusion in the Delta and San Francisco estuary through the 1960s (CDPW 1931; Hutton et al. 2015). The introduction of high-quality commercial salinometers in the 1970s led to the widespread use of conductivity as a measure of salinity, with the Practical Salinity Scale 1978 (Lewis 1980) being the international standard for reporting salinity values from conductivity measurements. Current research has recognized that there is a small numerical difference between practical salinity and the "absolute" salinity of seawater, which is defined as the mass of solids dissolved in solution per unit mass of seawater (Millero et al. 2008; Pawlowicz 2010; Wright et al. 2011).

Study Setting

Geographic Domain

The geographic focus of this paper is the San Francisco Estuary (Figure 1), which includes the delta formed by the Sacramento and San Joaquin rivers that consists of a network of islands and channels. The Delta is the entry point of over 90% of the freshwater inflow to San Francisco Bay (Cheng et al. 1993) and a major freshwater resource for California. Specifically, the Delta is the location of several water- withdrawal locations for municipal and agricultural use; some of these waters are exported across river-basin boundaries to support major urban and agricultural centers in the state (Lund et al. 2010). Several of the Delta islands are irrigated for agriculture and withdraw from and discharge water into the Delta. The natural and man-made system of the Delta is operated through major engineering components such as a system of reservoirs in the upper watershed, pump stations for export, and salt barriers to reduce salinity intrusion during low flow periods. The operation of this system adjusts to seasonal and interannual variations in hydrology, while meeting a complex set of water-quality and flow regulations intended to support environmental and human uses of the Delta waters (DSC 2013).

Sources of Salinity and Mixing within the Delta

The Delta is flat, with a dendritic network of channels and leveed islands with complex mixing over different time-scales (Monsen et al. 2007). The abundance of salinity constituents in Delta waters is affected by the relative volumes of saltwater from the ocean boundary, inflows from the major rivers, and agricultural discharges from Delta islands. Figure 2, which shows typical ionic compositions of major boundary source waters, highlights notable differences between seawater, freshwater inflows from the Sacramento River and smaller Sierra streams (e.g., Mokelumne and Cosumnes rivers), and inflows from the San Joaquin River.

Seawater, which is dominated by chloride and sodium, is approximately two orders of magnitude more saline than the upstream riverine source waters and exhibits nominal variability in ionic make-up and total concentration. Freshwater from the Sacramento River, which is dominated by bicarbonate, is characterized by larger proportions of calcium and magnesium, relative to seawater. Sacramento River salinity varies from approximately 50 to 150 mg L^{-1} TDS, with lower concentrations associated with high flow conditions and higher concentrations associated with low flow conditions. Compared with the other source waters, the San Joaquin River at

https://doi.org/10.15447/sfews.2023v21iss4art6

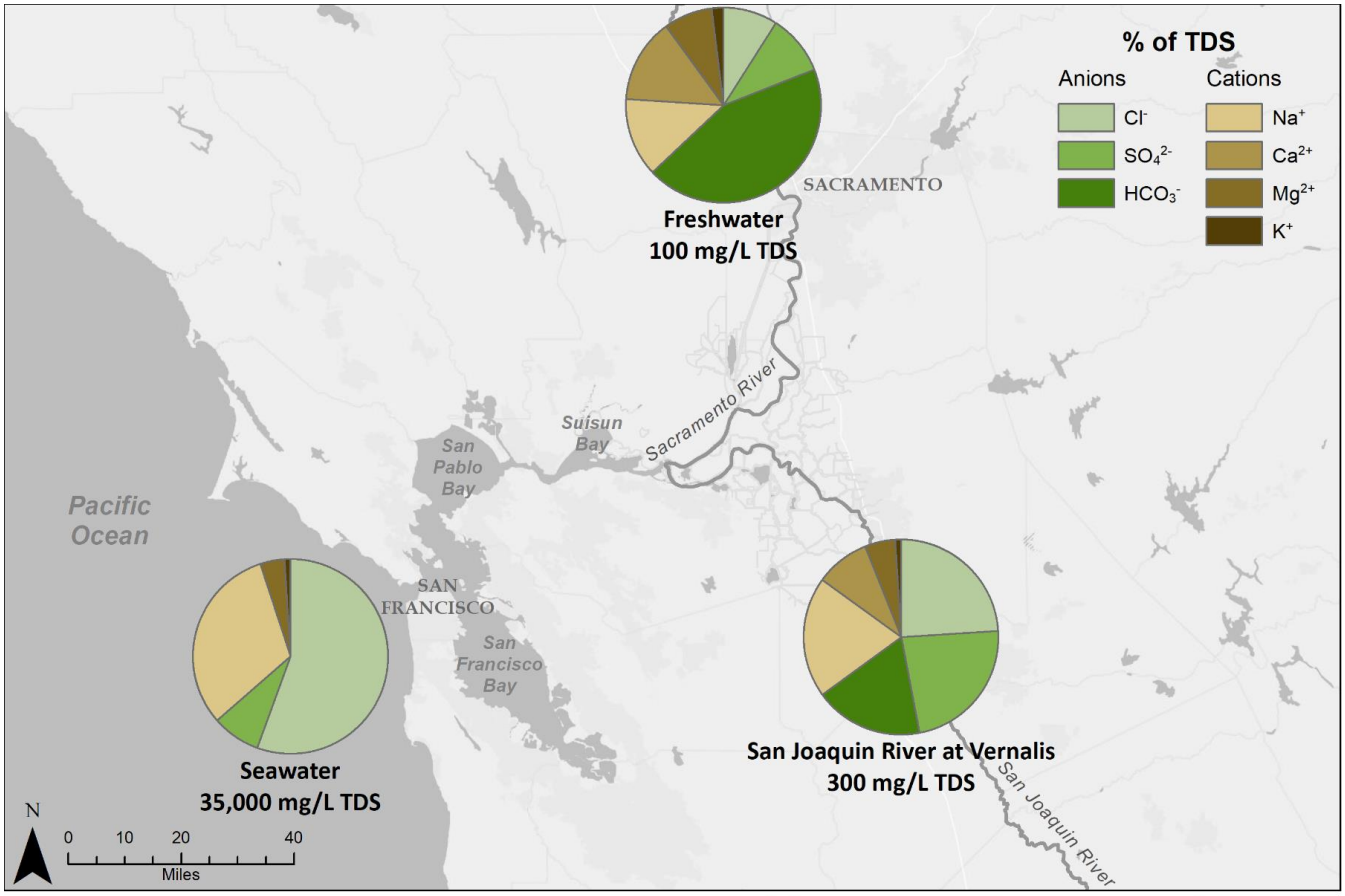

Service Layer Credits: Esri, HERE, Garmin, (c) OpenStreetMap contributors, and the GIS user community

Figure 2 Ionic composition of major boundary waters in the study region

Vernalis exhibits highly variable ionic make-up with salinity that ranges from approximately 100 to 600 mg L^{-1} TDS. Under high flow conditions, the ionic composition of the San Joaquin River reflects its low-salinity Sierra tributaries. Under lower flow conditions, depending on upstream reservoir operations, the San Joaquin River tends to be more influenced by high-salinity agricultural drainage. Water-quality regulations limit salinity at Vernalis to 700 µS cm^{-1} EC (400 mg L^{-1} TDS) between April and August and 1,000 µS cm^{-1} EC (600 mg L^{-1} TDS) in other months (CSWRCB 2000). In-Delta agricultural discharges (not shown in Figure 2) exhibit ionic compositions that vary, depending on location and timing of water withdrawals and discharges.

As a result of complex mixing, the contribution of different water sources to the ionic make-up at a given location in the study area varies over tidal cycles, seasonal wet and dry periods, and inter-annual wet and dry periods. Mixing over these different time-scales—which is governed by upstream hydrologic conditions as well as in-Delta hydrodynamic conditions—is influenced by natural climatic drivers as well as various anthropogenic influences. Given the typical source-specific ionic signatures (shown in Figure 2) and the variable contributions of these water sources at different locations, the relationship between salinity or TDS and individual ions is not a singular one in the Delta; rather, the relationship varies through space and time.

Previous Work

Pioneering work on estimating ionic and TDS concentrations from EC values in the estuary was reported in Guivetchi (1986). This work, based on a much smaller data set than currently

available, tabulated location-specific regression constants and statistics for estimating salinity concentrations assuming linear relationships between EC, chloride, and TDS. The tabulated regression constants were computed as functions of water year type to account for hydrologic variability. Over time, it became increasingly clear that the work's underlying conceptual model and statistical rigor was unable to account for seasonal changes in the relative contributions to salinity from different sources in much of the interior Delta. For example, Denton (1993) observed a bifurcated EC–chloride relationship at the Contra Costa Canal intake that varied with hydrology—it was characteristic of seawater when net flow conditions along the lower San Joaquin River were low, and characteristic of the San Joaquin River when net flow conditions were high. Hutton (2006, unreferenced, see "Notes") evaluated the co-occurrence of simulated source-water fingerprints and interior-Delta grab sample ion data; he noted distinct relationships between EC and ion concentrations that varied with the magnitude of simulated seawater and upstream source-water influences. More recently, Denton (2015) revisited the work of Guivetchi (1986) and reported statistical relationships for a broad suite of ions based on a more contemporary data set. His work is able to predict as well as our proposed methodology when estimating concentrations of salinity constituents in boundary regions; however, it is limited in its applicability to the interior Delta. Denton (2015) instead provides numerous potential methods to estimate salinity constituents, each of which we evaluated as we developed the proposed methodology in this study.

METHODS

Model formulation was supported by (1) compiling historically observed grab-sample salinity constituent data, (2) defining geographic grouping to characterize location-specific salinity relationships, and (3) following a data-screening protocol. These steps, along with standard statistical methods, are summarized below.

Data

We used grab sample data collected from waters in the study area to develop mathematical relationships between major salinity constituents of interest and EC. Our work considered the following salinity constituents: TDS, anions such as bromide (Br^-), chloride (Cl^-), sulfate (SO_4^{2-}), and bicarbonate (reported as alkalinity), and cations such as sodium (Na^+), calcium (Ca^{2+}), magnesium (Mg^{2+}), and potassium (K^+). We compiled an appropriate subset of grab-sample data from the CDWR Water Data Library (*https://wdl.water.ca.gov*) to characterize geographic-specific relationships between salinity constituents and to test the accuracy of the proposed methodology.

We supplemented the primary data source used here, which followed Denton's (2015) approach, with more recent data available in the CDWR Water Data Library. The monitoring locations that contribute grab-sample data to each of the geographic groupings are tabulated in Appendix A. Data used in this work span calendar years 1955 through 2021; however, most of these data were collected on or after the 1980s. To validate the proposed methodology, we obtained additional data from the Contra Costa Water District and the USGS's National Water Information System (NWIS). These data sources did not contain enough complete ion samples for us to consider their inclusion in the model-calibration process.

Geographic groupings, described below, were defined by regions where salinity data were hypothesized to exhibit similar inter-sample characteristics. Our hypotheses were based on domain knowledge of primary contributing sources of salinity, source-water mixing, and other seasonal or hydrological trends, and were confirmed through numerical source tracking using CDWR's Delta Simulation Model 2 (CDWR 2022).

Geographic Groupings

We defined two broad geographic groupings to characterize salinity constituent relationships: boundary regions and an interior Delta region

https://doi.org/10.15447/sfews.2023v21iss4art6

(see Figure 1). As described below, our modeling approach defined three boundary regions and classified the interior Delta region into three sub-regions.

The seawater boundary region is nominally bounded to the east by Emmaton along the Sacramento River and Jersey Point along the San Joaquin River (see Figure 1). This eastern demarcation provides a practical distinction with the upstream boundaries; however, we note that it is a somewhat fuzzy limit on the extent of seawater intrusion. Although the salinity gradient along the Sacramento River sharply trends from saline to fresh between Emmaton and Rio Vista (an upstream location) under typical low outflow conditions, the interface between seawater and freshwater characteristics can extend upstream of Emmaton, depending on hydrologic conditions. Similarly, the interface between seawater and freshwater characteristics can extend along the San Joaquin River upstream of Jersey Point. The seawater boundary region includes the Sacramento–San Joaquin River confluence area, Suisun Bay, San Pablo Bay, and San Francisco Bay.

The freshwater boundary region, which is nominally bounded to the south by the San Joaquin River, is commonly referred to as the North Delta and is primarily influenced by the Sacramento, Cosumnes, and Mokelumne rivers. We use data collected along the Sacramento River at Hood and Greene's Landing to characterize the freshwater boundary region. The Delta Cross Channel, while influencing the region's hydrology, has limited influence on its relative ionic make-up by affecting salinity intrusion on the Sacramento River during low flow periods. The Cache Slough Complex, although within the boundaries defined for this region, is highly influenced by its local watershed, and has distinct hydrology and geochemistry relative to the Sacramento, Cosumnes, and Mokelumne rivers. This distinction is significant, because the North Bay Aqueduct (part of the SWP) diverts water from Barker Slough within this complex. We developed unique statistical relationships between EC, TDS, and ionic concentrations for this urban diversion as part of this work, which are reported in Hutton et al. (2022b).

The San Joaquin River boundary region is characterized by the namesake river at Vernalis. Salinity characteristics of San Joaquin River inflow to the Delta are dominated by agricultural drainage from the west side of the valley, except for periods of unusual runoff conditions from the high Sierra.

The interior Delta region exhibits composite characteristics of the boundary regions that vary with season and hydrology. This region is nominally bounded by the freshwater boundary region to the north, the seawater boundary region to the west, and the San Joaquin River boundary region to the south. The region was further divided into three sub-regions to reflect unique source-water influences that vary by hydrology and season: Old and Middle River export corridor, San Joaquin River corridor, and the South Delta. Sub-region boundaries and grab-sample locations used to represent each sub-region are identified in Figure 3. Within the interior Delta region, the Old and Middle River export corridor sub-region is uniquely influenced by hydrodynamic patterns driven by the SWP and CVP export operations at the Harvey O. Banks and C. W. "Bill" Jones pumping plants, respectively. The San Joaquin River corridor sub-region is uniquely influenced by salinity conditions at Vernalis. The South Delta sub-region is uniquely influenced by salt loads that enter the Delta at Vernalis, the placement of seasonal in-channel rock barriers (Hutton et al. 2019; Kimmerer et al. 2019), and local sources of salinity (including agricultural drainage and groundwater) (Montoya 2007).

Data Screening

Data samples selected to represent the boundary regions were screened for "testability." We defined testable data samples as those that had measured values for each of the following constituents: EC, TDS, key anions (Cl^- and SO_4^{2-}), and key cations (Na^+ and Mg^{2+}). Testability was enforced to ensure that samples were reasonably mass- and charge-balanced. After the "testability" check, we imposed two additional screening

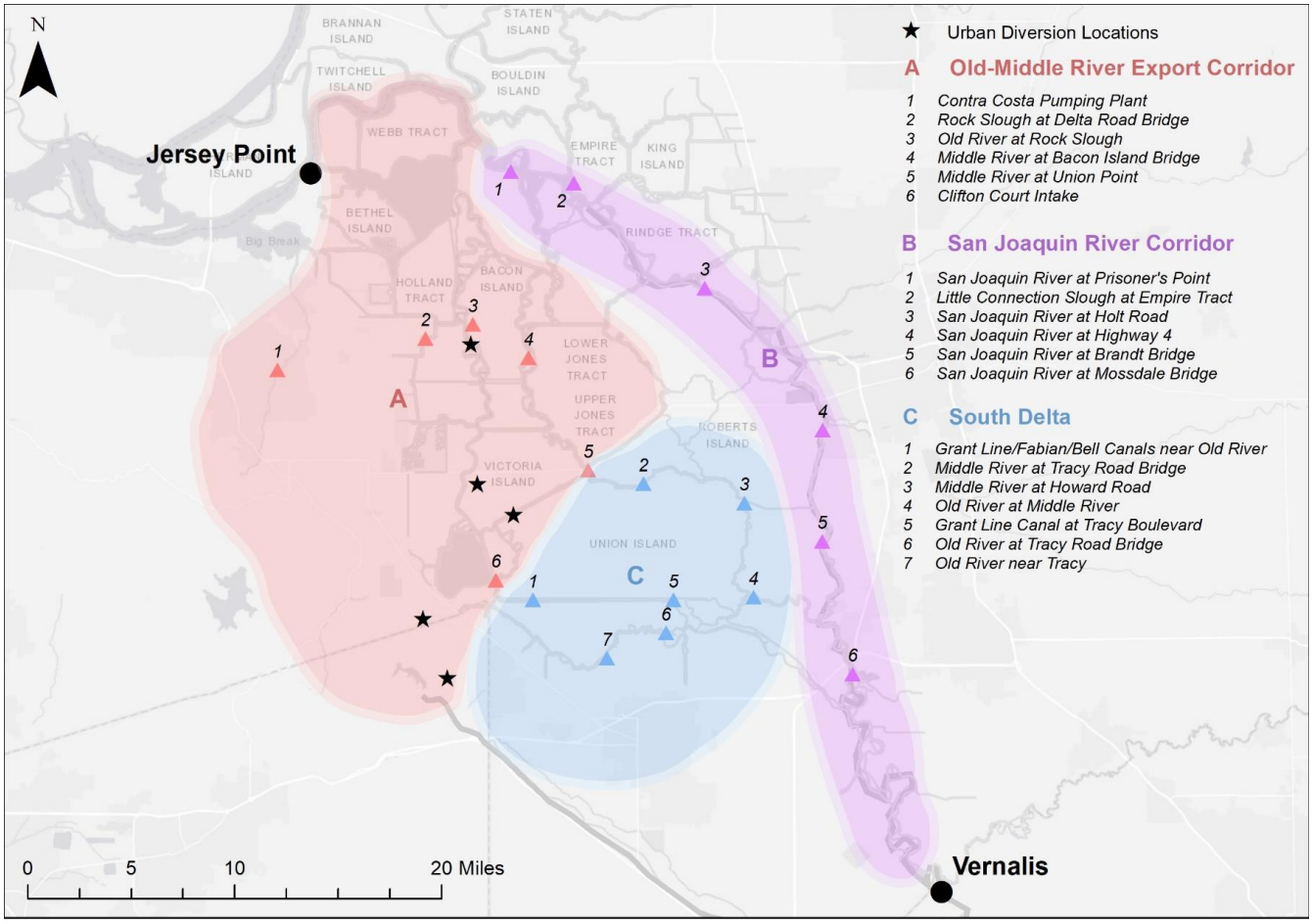

Service Layer Credits: Esri, HERE, Garmin, (c) OpenStreetMap contributors, and the GIS user community

Figure 3 Delineation of three sub-regions in the interior Delta and associated water quality sampling stations. *Symbols, numbers, and colors* indicate the locations of water quality sampling stations and major urban water diversions.

criteria on the boundary region data sets: (1) A data point associated with a single constituent was removed if, when plotted against EC or TDS, it fell outside the 99% prediction band (three standard deviations) for the testable set of observations for that constituent, and (2) an entire sample, including all data points associated with it, was removed if three or more constituents in that sample fell outside the 95% prediction band (two standard deviations) for the testable set of observations for the constituents.

Because the boundary regions exhibited strong, year-round characteristics of seawater, freshwater, or San Joaquin River dominance—regardless of season or hydrologic conditions—these screening criteria removed anomalous data and samples and preserved dominant characteristics. We excluded the following data in adherence to the 99% prediction-band criteria: 38 constituent values (from 36 samples) associated with the seawater boundary region, 51 constituent values (from 46 samples) associated with the freshwater boundary region, and 41 constituent values (from 39 samples) associated with the San Joaquin River boundary region. In adherence to the 95% prediction-band criteria, we excluded 35 samples associated with the seawater boundary region, 42 samples associated with the freshwater boundary region, and 67 samples associated with the San Joaquin River boundary region. Excluded values exhibited neither temporal clustering nor seasonal patterns. However, very few TDS and Cl^- values were excluded (relative to the other

https://doi.org/10.15447/sfews.2023v21iss4art6

constituents) in adherence to the 99% prediction-band criteria.

The data set used to represent salinity constituent relationships in the interior Delta region demonstrated greater scatter when compared to the data sets used to represent the boundary regions. In recognition of this greater scatter and given a desire to conserve sample size, no testability or data- screening criteria were imposed on the interior Delta region data set.

Model Formulation and Statistical Methods

Below, we discuss distinguishing aspects that are associated with formulating ion–EC relationships for the boundary regions and the interior Delta region. Model equations and associated constants use EC as the independent variable to predict TDS and ion concentrations of interest, including four anions (Br^-, Cl^-, SO_4^{2-}, HCO_3^-) and four cations (Na^+, Ca^{2+}, Mg^{2+}, K^+). As previously noted, we use alkalinity (reported in units of mg L^{-1} as $CaCO_3$) in this work as a proxy measure for HCO_3^-.

Seawater Boundary Region

Relationships between ions, TDS, and EC within the seawater boundary region were based on an extension of the Practical Salinity Scale 1978 (Lewis 1980) applying the assumption of steady-state, two-source conservative mixing, and specifying appropriate values for upstream and downstream end-member properties. Results are summarized later in this paper; however, methodological details are provided elsewhere (Hutton et al. 2022b; Hutton and Roy 2023b).

Freshwater and San Joaquin River Boundary Regions

Screened data sets were used to calibrate unique regression equations that depict the salinity constituent relationships exhibited within these boundary regions, given that the assumption of two-source conservative mixing (as applied to the seawater boundary region) did not appear to be valid because (1) grab-sample data for the freshwater boundary region (measured along the Sacramento River at Hood and Greene's Landing) varied over a narrow conductivity range of 50 to 250 µS cm^{-1} and showed little variation in ionic proportions, suggesting a single dominant source of salinity, and (2) grab-sample data for the San Joaquin River boundary region varied over a much broader conductivity range but showed non-linear relationships between ions, suggesting more than two dominant sources of salinity at Vernalis. Following Denton (2015), an ordinary least-squares approach was generally used for both boundary regions to determine the regression constants *A*, *B*, and *C* in the quadratic equation:

$$Y = A * EC^2 + B * EC + C \quad \text{Eq 1}$$

where *Y* is the dependent variable of interest.

Interior Delta Region

As noted earlier, the interior Delta region exhibits composite characteristics of the boundary regions that vary with season and hydrology. Denton (2015) observed that the ion–EC relationships associated with waters in this region are generally bounded by the seawater and San Joaquin River boundary relationships. Our modeling approach employs a decision tree (and associated matrices) that prescribes a dominant source water based on the following simplified hydrodynamic proxies: month, water year type, and (optionally) position of the 2 ppt bottom salinity isohaline commonly referred to as X2 (Hutton et al. 2015).

To develop this decision tree, we performed an extensive assessment of EC, TDS and major ion relationships across the region grouped by month, water year, and X2 position. We defined the X2 threshold at the longitudinal distance associated with the Collinsville monitoring location (X2 = 81 km) as a broad indicator of saltwater intrusion into the Delta. This location plays a key regulatory role in the management of X2 in spring and fall (Hutton et al. 2015). The goal of this decision tree assessment was to identify data groupings that most closely aligned with either the seawater or San Joaquin River ionic relationships. The groupings were also confirmed through prior knowledge of system dynamics and through review of numerical modeling results. The X2 threshold was not continuously

varied to evaluate the sensitivity of the groupings developed.

While flow-based hydrodynamic proxies may be more conceptually appealing, we did not explore such an approach, because such proxies would need to relate salinity intrusion to complex time-histories of one or more flows, thereby conflicting with our objective of developing a simplified approach targeted toward a broad stakeholder community. (We note that water year type is itself a categorical summary of the time-history of flows and other inputs.) We computed both R^2 and standard error (*SE*) statistics to evaluate the methodology's goodness-of-fit to data observed in the interior Delta region.

Model Validation

We note that, while separate calibration and validation steps are generally part of a sound modeling protocol (Roy et al. 2021), an explicit validation step for all the equations developed is of secondary importance for this work and is not reported here in the interest of brevity. In support of this opinion, we note that the scientific basis for relating ionic concentrations to EC is well-understood, transparent, and highly constrained by mass and charge balances. Notwithstanding, we used long-term co-located EC, TDS and major ion data collected by the USGS along the Sacramento and San Joaquin Rivers to validate corresponding boundary relationships. Similarly, we report a validation of the EC–Cl^- relationship in the Old and Middle River export corridor using an independent 20-year data set collected by the Contra Costa Water District at their Old River intake. The interested reader is also referred elsewhere for additional validation analysis (Hutton et al. 2022b) that used data screened from the calibration process.

Trend Analysis

Time-series trends (spanning nearly a century) and change attribution have been reported for flows—both tidally-averaged in the interior Delta (Hutton et al. 2019) and freshwater flow to the estuary (Hutton et al. 2017a, 2017b)—as well as for salinity (Hutton et al. 2015). We did not observe commensurate time-series trends in the boundary relationships between ionic concentrations and EC; however, as we have no basis for hypothesizing that such trends may exist over the available period of record, we did not conduct formal trend analyses. One noteworthy exception relates to a step change observed at the San Joaquin River boundary. Data collected before 1982, while not used in our work (see Appendix A), reflect a higher chloride-to-sulfate ratio than the post-1982 data (Denton 2015). The pre-1982 ionic make-up was influenced by the accretion of saline water from gas wells along the Tuolumne River upstream of Vernalis (SDWA 1980; Kratzer and Grober 1991); these wells were later capped (Denton 2015).

Similarly, we did not observe commensurate ion–EC time-series trends in the interior Delta, nor did we conduct formal trend analyses. However, unlike the boundary regions, we hypothesize that relationships with season, water year type, and X2 have in fact changed over the past century, but that such relationships have been relatively stationary since the 1970s, after construction of major upstream reservoirs and Delta export facilities as well as implementation of environmental regulations. While such a hypothesis could be explored through hydrodynamic modeling, (1) little observed data exists to validate, and (2) such an effort is outside the scope of this work.

RESULTS

Decision Tree

Given a location-specific value of EC and knowledge of the sampling period and region, we developed a decision tree (Figure 4) following the methodology described earlier to help users select the appropriate set of model constants to estimate the salinity constituent(s) of interest. In the simplest case, an EC value associated with a boundary region (i.e., seawater, freshwater, or San Joaquin River) can be converted to a salinity constituent concentration by applying the logic shown in Branch 1 of the decision tree (i.e., using the corresponding boundary regression relationships). Similarly, an EC value associated with the interior Delta region can be converted to

https://doi.org/10.15447/sfews.2023v21iss4art6

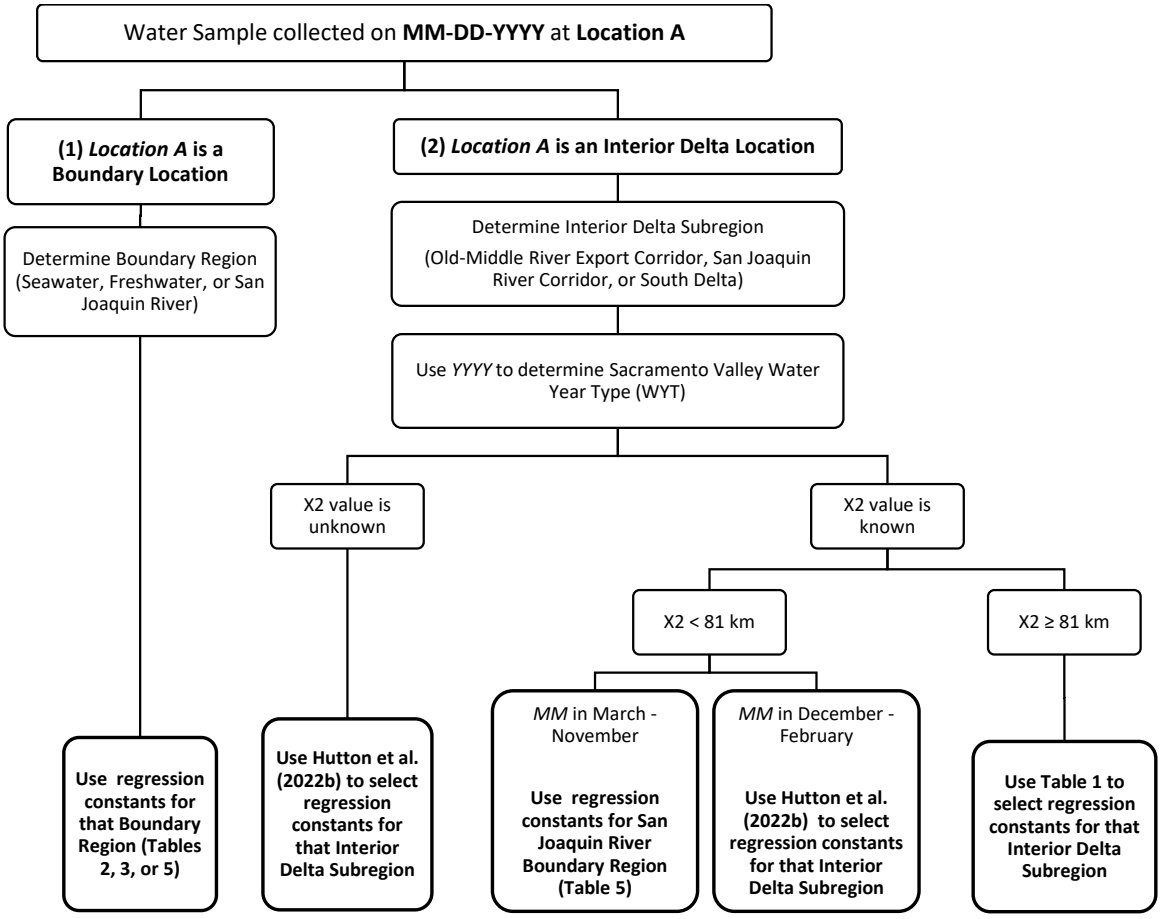

Figure 4 This decision tree was developed to assist users in selecting the appropriate set of model constants for estimating salinity constituent(s) of interest given a location-specific value of *EC* and knowledge of the sampling period and region.

a constituent concentration by applying the logic shown in Branch 2 of the decision tree. This more complicated logic accounts for seasonal changes in the relative contributions from different sources to water quality through proxy inputs. For this branch, required user inputs include location (i.e., interior Delta sub-region), month, and water year type, with X2 position being an optional user input.

An exploration of the data sets compiled for each of the interior Delta sub-regions showed that their salinity characteristics were either akin to the seawater boundary, the San Joaquin River boundary, or an indeterminate mixture of source waters. In most instances, hydrologic proxies (i.e., sampling month, water year type, and X2 position) provided sufficient information to discriminate between data samples with stronger seawater characteristics and data samples with stronger San Joaquin River characteristics. However, a subset of interior Delta samples associated with the San Joaquin River corridor and the South Delta sub-regions exhibited indeterminate source characteristics. We developed unique regression relationships to characterize this data subset; model constants and fitting statistics are reported in Appendix B. Table 1 shows the relationship between source water dominance and proxy inputs for each interior Delta sub-region when X2 position is known and ≥ 81 km. A similar table is provided in Hutton et al. (2022b, Table 11) when X2 position is unknown or < 81 km.

A nuanced aspect of the decision tree logic is found along Branch 2 when the X2 value is

known. Typically, winter reservoir operations and unregulated runoff translate into higher river flows; these higher flows flush salts that have intruded into the western Delta near the location of the Sacramento and San Joaquin River confluence during the preceding summer and fall months. Under these conditions, although salinity is pushed downstream (with X2 nominally < 81 km), salts may remain trapped in the interior Delta for several weeks or months. To account for this recurring hydrodynamic phenomenon, the decision tree provides additional seasonally dependent guidance on determining dominant source water and resulting model constants.

Boundary Regions

Here, we summarize results of our work to estimate TDS and ion concentrations as functions of EC for the seawater, freshwater, and San Joaquin River boundary regions. Reported goodness-of-fit statistics include (1) the coefficient of determination (R^2), a dimensionless measure of the proportion of the variance in the dependent variable that is explained by the independent variable, and (2) the standard error (*SE*), the statistical accuracy of the estimate expressed in units of the dependent variable. Parameter uncertainties were calculated for model constants determined through ordinary least-squares regression and are reported in Hutton et al. (2022b).

Seawater Boundary Region

Seawater enters the study domain through tidal action at the Golden Gate (see Figure 1). Two salinity ranges ("low" and "high" salinity) were defined to divide the spectrum of observed and expected values of EC because the constituent relationships were found to have unique trends which a single model fit could not adequately capture. Under "low" salinity conditions ($EC < 250\,\mu S\,cm^{-1}$), waters in the region overwhelmingly reflect characteristics of upstream freshwater flows, and do not reflect seawater mixing. Following the polynomial form of the Practical Salinity Scale 1978 (Lewis 1980; Schemel 2001), constituent relationships are captured for both salinity ranges by the constants and statistics in Table 2.

Data fits for the high-salinity range are very good ($R^2 > 0.98$) for all constituents except alkalinity. Although conservative mixing between seawater and freshwater end-members plays an important role in controlling the alkalinity distribution in estuaries, biogeochemical sources and sinks are recognized (Najjar et al. 2019). Hutton and Roy (2023b) observed that the poorer alkalinity predictions are seasonally biased (under-predicted in December through June and over-predicted in July through November) and are extremely sensitive to the assumed upstream end-member concentration. Data fits for the low-salinity range are poorer, with R^2 values for Br^-, SO_4^{2-} and K^+ less than 0.70.

Freshwater Boundary Region

Freshwater inflows from the Sacramento, Cosumnes, and Mokelumne rivers dominate the salinity characteristics of the freshwater boundary region, a significant area of the Delta above (i.e., north of) the San Joaquin River. The relationships between salinity constituents measured along the Sacramento River are used to characterize the freshwater boundary region and are captured by the constants and statistics in Table 3. The intercept term of the regression equations (the term *C* in Equation 1) was set to zero for all constituents except TDS to constrain predictions to non-negative values. Data fits for this region are mixed, with $R^2 > 0.9$ for TDS, alkalinity, and Na^+ and $R^2 < 0.7$ for Br^- and K^+. Measured concentrations of Br^- never exceeded 0.03 mg L^{-1}, well below the constituent's detection limit.

We compared the freshwater boundary-region regression relationships with a long record (1960–2022) of co-located EC, TDS, and major ion data collected by the USGS along the Sacramento River at Freeport. Goodness-of-fit statistics, provided in Table 4, are consistently poorer than for the calibration data set. Modeled relationships systematically under-predicted concentrations of TDS, Ca^{2+}, and Mg^{2+}. We note that the Freeport monitoring location is several miles upstream of Sacramento River monitoring locations (i.e., Hood and Greene's Landing) used for model calibration.

https://doi.org/10.15447/sfews.2023v21iss4art6

San Joaquin River Boundary Region

San Joaquin River inflow to the Delta at Vernalis, which is a mixture of freshwater runoff from the Sierra Nevada range and high-salinity agricultural drainage from the west side of the San Joaquin Valley, greatly influences salinity in the sub-regions of the interior Delta. The relationships between salinity constituents measured at or near this location are used to characterize the San Joaquin River boundary region and are captured by the constants and statistics in Table 5. Data fits are very good, with $R^2 > 0.94$ for all constituents except K^+.

The San Joaquin River boundary-region regression relationships were compared with a long record (1982–2022) of co-located EC, TDS, and major ion data collected by the USGS at Vernalis. Goodness-of-fit statistics, provided in Table 6, are generally like those reported for the calibration data set. However, the K^+ data exhibited significant scatter and thus showed poorer goodness-of-fit with the calibrated relationships.

Interior Delta Region

Here, we summarize the results of our work to estimate TDS and ion concentrations as functions of EC for the interior Delta region.

Old and Middle River Export Corridor Sub-Region

The decision-tree approach provided mixed results in terms of fitting to observed TDS and ion data in the Old and Middle River export corridor sub-region of the interior Delta (see Table 7). Calculated statistics assume availability of X2 data. Data fits are good ($R^2 \geq 0.90$) for TDS, Cl^-, Na^+ and Mg^{2+} and are poor ($R^2 < 0.70$) for Br^-, SO_4^{2-}, alkalinity, and Ca^{2+}.

Source-water dominance in the interior Delta sub-region varies by month, water year type, and X2 position. When X2 position is ≥ 81 km (see Table 1), the seawater boundary is always prescribed as the dominant source water during the months of September through January. The top panel of Figure 5, which presents a scatter plot of Cl^- as a function of EC at Banks Pumping Plant, illustrates observed and predicted bi-modal source-water dominance. The observed data were assigned a source-water dominance following Table 1; these assignments generally align with and are bounded by the predicted San Joaquin River and seawater boundary relationships. The bottom panel of Figure 5 presents a similar scatter plot at Banks Pumping Plant; however, in this panel the observed data were assigned a source- water dominance using daily-averaged, DSM2-simulated source-tracking data to predict seawater boundary influence following Hutton (2006, unreferenced, see "Notes"). Observed data assigned to a simulated seawater boundary influence > 0.4% generally fall along the predicted seawater boundary relationship, while those observed data assigned to a simulated seawater boundary influence < 0.4% generally fall along the predicted San Joaquin River boundary relationship. This alternate data assignment provides nearly identical results to the top panel and lends confidence to the use of the decision-tree approach as a simplified proxy for interior Delta hydrodynamic conditions. We further observed that data scatter around the predicted seawater boundary relationship in the bottom panel of Figure 5 could be reduced through additional parsing by DSM2-simulated Sacramento River boundary influence. Further analysis of the influence of upstream boundary influences on EC–ion relationships is beyond the scope of this work and was not undertaken.

Observed Cl^- data at Banks Pumping Plant are presented in Figure 6 as a time-series for the 3-year period that spanned October 2014 through September 2017. Generally bounding the observed data are EC-based predictions of Cl^- concentration, assuming seawater and San Joaquin River boundary relationships. The chart further delineates periods of seawater dominance and San Joaquin River dominance.

Figure 7 provides a time-series comparison of observed and predicted Cl^- data at the Contra Costa Water District intake along Old River (located in Figure 1 as Old River at Highway 4). The independent EC and Cl^- time-series, which span 20 years between January 2001 and December 2020, afford a unique validation of the decision-tree approach, given the length

Table 1 Water year type and season matrix. This matrix can be used to select the appropriate interior Delta salinity relationship when X2 position is known and is ≥ 81 km. The rows denote the water year types and the columns denote months of the year. For each interior Delta sub-region, the cell that represents a particular month and water year type combination shows the dominant boundary influence: San Joaquin River (SJR), Seawater (SEA), or indeterminate (IND). Model constants and statistics corresponding to the dominant boundary influence can be used to estimate the salinity constituents. Water year types can be wet (W), above normal (AN), below normal (BN), dry (D), or critical (C).

	J	F	M	A	M	J	J	A	S	O	N	D
Old and Middle River export corridor sub-region												
W	SEA	SJR	SJR	SJR	SJR	SJR	SJR	SJR	SEA	SEA	SEA	SEA
AN	SEA	SJR	SJR	SJR	SJR	SJR	SJR	SJR	SEA	SEA	SEA	SEA
BN	SEA	SEA	SEA	SEA	SEA	SEA	SEA	SEA	SEA	SEA	SEA	SEA
D	SEA	SEA	SEA	SEA	SEA	SEA	SEA	SEA	SEA	SEA	SEA	SEA
C	SEA	SEA	SEA	SEA	SEA	SEA	SEA	SEA	SEA	SEA	SEA	SEA
San Joaquin River corridor sub-region												
W	SJR	SJR	SJR	SJR	SJR	SJR	SJR	SJR	SJR	SJR	SJR	SJR
AN	SJR	SJR	SJR	SJR	SJR	SJR	SJR	SJR	SJR	SJR	SJR	SJR
BN	SJR	SJR	SJR	SJR	SJR	SJR	SJR	SJR	SJR	SJR	SJR	SJR
D	SJR	SJR	SJR	SJR	SJR	SJR	SJR	SJR	SJR	SJR	SJR	SJR
C	SJR	SJR	SJR	SJR	SJR	SJR	SJR	SJR	SJR	SJR	SJR	SJR
South Delta sub-region												
W	SJR	SJR	SJR	SJR	SJR	SJR	SJR	SJR	SJR	SJR	SJR	SJR
AN	SJR	SJR	SJR	SJR	SJR	SJR	SJR	SJR	SJR	SJR	SJR	SJR
BN	IND	IND	SJR	SJR	SJR	SJR	SJR	IND	IND	IND	IND	IND
D	IND	IND	SJR	SJR	SJR	SJR	SJR	IND	IND	IND	IND	IND
C	IND	IND	SJR	SJR	SJR	IND	IND	IND	IND	IND	IND	IND

and frequency (daily) of a measured ionic constituent in the study area. This comparison shows generally good predictive capability of the approach over a wide range of hydrologic conditions, with EC values ranging from 73 to 938 μS cm^{-1} and Cl^- values ranging from 8 to 194 mg L^{-1}. Under predicted seawater-dominant conditions when EC ≥ 250 μS cm^{-1}, the standard error of estimate was 14.0 mg L^{-1} (Cl^- average = 100 mg L^{-1}); under predicted seawater-dominant conditions when 100 μS cm^{-1} < *EC* < 250 μS cm^{-1}, the standard error of estimate was 8.4 mgL^{-1} (Cl^- average = 25 mg L^{-1}); under predicted San Joaquin River-dominant conditions, the standard error of estimate was 8.9 mg L^{-1} (Cl^- average = 34 mg L^{-1}). We suspect that the EC time-series is corrupt over a wet period that spanned February 16, 2017 through March 10, 2017 (when the location was expected to reflect San Joaquin River dominance), given an abrupt and otherwise unexplainable drop in EC from 915 μS cm^{-1} to 396 μS cm^{-1} between March 8 and March 9. Following this observation, the latter goodness-of-fit estimate excluded these suspicious data.

San Joaquin River Corridor and South Delta Sub-Regions

The decision-tree approach generally provided good fits to observed TDS and ion data in the San Joaquin River corridor and South Delta sub-regions of the interior Delta. Table 7 presents fitting statistics for both sub-regions. Calculated statistics assume availability of X2 data. The San Joaquin River boundary is generally prescribed as the dominant source water in both sub-regions for all months, water year types, and X2 conditions (see Table 1 when X2 ≥ 81 m). In the San Joaquin River corridor sub-region, $R^2 > 0.90$ for all constituents except alkalinity ($R^2 = 0.77$) and K^+ ($R^2 = 0.36$). In the South Delta sub-region,

https://doi.org/10.15447/sfews.2023v21iss4art6

Table 2 Model constants and statistics (seawater boundary). These tables can be used to estimate salinity constituents of interest within the seawater boundary region given a known value of *EC*. Each row represents one relationship and contains the model constants (*K1* through *K6*) in the polynomial equation $Y = K1 + K2\,[EC]^{0.5} + K3\,[EC] + K4\,[EC]^{1.5} + K5\,[EC]^{2} + K6\,[EC]^{2.5}$, that are used to estimate *Y*, the concentration of the salinity constituent of interest. The seawater boundary region is divided into two salinity ranges: low and high. Units are mg L^{-1} for all constituents. For alkalinity, units are expressed as mg L^{-1} as $CaCO_3$.

X = EC	*Y*	Data points	*K1*	*K2*	*K3*	*K4*	*K5*	*K6*	R^2	*SE*	Data range
"Low" salinity 100 ≤ [EC] < 250 µS cm^{-1}	**TDS**	60	−1.29E + 01	−9.85E − 01	8.68E − 01	1.19E − 03	−7.73E − 04	4.28E − 09	0.953	4.6	67 – 151
	Br^-	59	1.47E − 01	−1.82E − 03	−1.48E − 03	2.21E − 06	5.28E − 06	7.93E − 12	0.666	0.01	0.01 – 0.1
	Cl^-	61	1.87E + 01	−5.34E − 01	−1.32E − 01	6.47E − 04	7.28E − 04	2.32E − 09	0.834	2.2	7 – 31
	SO_4^{2-}	61	−7.88E + 00	−7.20E − 02	1.46E − 01	8.72E − 05	−1.67E − 04	3.13E − 10	0.547	2.3	6 – 22
	Alkalinity	61	3.46E + 00	−1.42E − 03	3.20E − 01	1.72E − 06	−2.62E − 04	6.18E − 12	0.708	4.6	37 – 72
	Na^+	61	1.08E + 01	−2.88E − 01	−4.57E − 02	3.49E − 04	4.12E − 04	1.25E − 09	0.911	1.1	7 – 22
	Ca^{2+}	61	−6.95E + 00	−1.11E − 02	1.66E − 01	1.34E − 05	−3.32E − 04	4.81E − 11	0.731	0.9	8 – 16
	Mg^{2+}	61	−3.03E + 00	−3.51E − 02	7.26E − 02	4.25E − 05	−9.44E − 05	1.52E − 10	0.840	0.5	4 – 9
	K^+	61	6.79E − 01	−1.10E − 02	5.60E − 03	1.33E − 05	−2.74E − 08	4.77E − 11	0.161	0.3	0.9 – 2.5
X = EC	*Y*	Data points	*K1*	*K2*	*K3*	*K4*	*K5*	*K6*	R^2	*SE*	Data range
"High" salinity [EC] ≥ 250 µS cm^{-1}	**TDS**	344	3.05E + 01	−9.85E − 01	5.02E − 01	1.19E − 03	−2.46E − 06	4.28E − 09	0.997	173	151 – 11,630
	Br^-	299	−1.25E − 01	−1.82E − 03	9.29E − 04	2.21E − 06	−4.54E − 09	7.93E − 12	0.986	0.7	0.07 – 20
	Cl^-	343	−3.67E + 01	−5.34E − 01	2.72E − 01	6.47E − 04	−1.33E − 06	2.32E − 09	0.998	83	23 – 6,044
	SO_4^{2-}	339	9.08E + 00	−7.20E − 02	3.67E − 02	8.72E − 05	−1.79E − 07	3.13E − 10	0.994	18	14 – 853
	Alkalinity	338	6.68E + 01	−1.42E − 03	7.25E − 04	1.72E − 06	−3.54E − 09	6.18E − 12	0.381	8.6	41 – 96
	Na^+	340	−1.15E + 01	−2.88E − 01	1.47E − 01	3.49E − 04	−7.18E − 07	1.25E − 09	0.997	46	21 – 3,298
	Ca^{2+}	341	1.23E + 01	−1.11E − 02	5.64E − 03	1.34E − 05	−2.76E − 08	4.81E − 11	0.989	3.7	9 – 143
	Mg^{2+}	336	4.76E + 00	−3.51E − 02	1.79E − 02	4.25E − 05	−8.73E − 08	1.52E − 10	0.993	9.2	8.94 – 424
	K^+	339	6.79E − 01	−1.10E − 02	5.60E − 03	1.33E − 05	−2.74E − 08	4.77E − 11	0.984	4.4	1.90 – 134

Table 3 Model constants and statistics (freshwater boundary). This table can be used to estimate salinity constituents of interest within the freshwater boundary region given a known value of *EC*, when it ranges from 50 to 250 µS cm^{-1}. Each row represents one relationship and contains the regression constants (*A*, *B*, *C*) in the quadratic equation $Y = A\,[EC]^2 + B\,[EC] + C$, that are used to estimate *Y*, the concentration of the salinity constituent of interest. Units are mg L^{-1} for all constituents. For alkalinity, units are expressed as mg L^{-1} as $CaCO_3$.

Y	Data points	*A*	*B*	*C*	R^2	*SE*	Data range
TDS	600	1.21E − 04	0.503	13.2	0.923	5.2	44 – 151
Br^-	377	8.51E − 08	7.61E − 05	0	0.236	0.01	0 – 0.03
Cl^-	598	1.26E − 04	0.0194	0	0.816	0.9	2 – 13
SO_4^{2-}	595	1.20E − 04	0.0277	0	0.727	1.3	2 – 17
Alkalinity	591	− 3.67E − 04	0.442	0	0.916	3.3	24 – 88
Na^+	594	1.22E − 04	0.0408	0	0.902	0.9	3 – 17
Ca^{2+}	596	−1.28E − 04	0.0952	0	0.828	0.8	6 – 17
Mg^{2+}	596	5.77E − 06	0.0398	0	0.892	0.5	3 – 10
K^+	591	−1.27E − 05	0.0105	0	0.422	0.2	0.6 – 2.2

Table 4 Freshwater boundary model validation statistics for the USGS Sacramento River Station at Freeport (11447650)

Y	Data points	R^2	*SE*	Data range
TDS	543	0.698	11.9	37 – 169
Br–	0	N/A	N/A	N/A
Cl^-	543	0.766	1.2	1 – 15
SO_4^{2-}	543	0.405	2.6	1 – 22
Alkalinity	52	0.791	5.6	31 – 85
Na^+	543	0.866	1.2	2 – 21
Ca^{2+}	543	0.728	1.2	5 – 19
Mg^{2+}	543	0.859	0.6	2 – 12
K^+	540	0.194	0.3	0.5 – 2.7

Table 5 Model constants and statistics (San Joaquin River boundary). This table can be used to estimate salinity constituents of interest within the San Joaquin River boundary region given a known value of *EC*, when it ranges from 100 to 1,600 µS cm^{-1}. Each row represents one relationship and contains the regression constants (*A, B, C*) in the quadratic equation $Y = A\,[EC]^2 + B\,[EC] + C$, that are used to estimate *Y*, the concentration of the salinity constituent of interest. Units are mg L^{-1} for all constituents. For alkalinity, units are expressed as mg L^{-1} as $CaCO_3$.

Y	Data points	*A*	*B*	*C*	R^2	*SE*	Data range
TDS	543	5.73E – 05	0.526	11.3	0.997	10.7	75 – 1070
Br–	458	2.70E – 08	0.000458	– 0.05	0.941	0.03	0.02 – 0.74
Cl^-	541	6.50E – 06	0.147	– 12.5	0.989	5.2	7 – 242
SO_4^{2-}	542	4.76E – 05	0.0917	3.8	0.968	9.3	10 – 304
Alkalinity	541	– 4.01E – 05	0.162	9.5	0.946	7.8	29 – 181
Na^+	537	1.24E – 05	0.110	– 3.9	0.992	3.5	10 – 217
Ca^{2+}	534	2.41E – 06	0.0420	3.4	0.979	2.1	8 – 82
Mg^{2+}	538	2.44E – 06	0.0232	0.5	0.985	1.0	3 – 46
K^+	530	3.78E – 07	0.00232	1.0	0.803	0.4	0.5 – 6.2

Table 6 San Joaquin River boundary model validation statistics for the USGS Station at Vernalis (Station 11303500)

Y	Data points	R^2	*SE*	Data range
TDS	523	0.977	24.3	51 – 826
Br–	0	N/A	N/A	N/A
Cl^-	523	0.967	7.7	5 – 200
SO_4^{2-}	523	0.917	12.9	5 – 240
Alkalinity	68	0.790	13.8	26 – 167
Na^+	523	0.972	5.7	6 – 170
Ca^{2+}	523	0.953	2.5	6 – 66
Mg^{2+}	523	0.960	1.3	2 – 33
K^+	516	0.324	1.0	0.9 – 11

https://doi.org/10.15447/sfews.2023v21iss4art6

Table 7 Statistical fits (R^2 and Standard Error [*SE*]) associated with constituent estimates for the three interior Delta sub-regions. As demonstrated in Figure 4 (Branch 2), given *EC* observations, sampling month, water year type, and (optionally) X2 position, the appropriate water year type and season matrix (e.g., Table 1) can be consulted to determine the dominant boundary influence. Units are mg L^{-1} for all constituents. For alkalinity, units are expressed as mg L^{-1} as $CaCO_3$.

X = EC	*Y*	Data points	R^2	*SE*	Data range
Old and Middle River export corridor	**TDS**	753	0.992	15.3	73 – 900
	Br^-	594	0.453	0.2	0.03 – 5.35
	Cl^-	1057	0.958	16.7	5.9 – 511
	SO_4^{2-}	507	0.644	13.6	8 – 195
	Alkalinity	510	0.353	12.3	27 – 153
	Na^+	957	0.986	5.0	8.5 – 250
	Ca^{2+}	769	0.410	3.9	8 – 45.2
	Mg^{2+}	770	0.896	1.8	3 – 40
	K^+	624	0.758	0.7	0.9 – 10
San Joaquin River corridor	**TDS**	274	0.978	23.3	49 – 852
	Br^-	99	0.922	0.04	0.02 – 0.6
	Cl^-	352	0.913	14.3	4 – 260
	SO_4^{2-}	98	0.932	14.6	5 – 235
	Alkalinity	224	0.772	14.2	30 – 198
	Na^+	149	0.982	5.6	7 – 167
	Ca^{2+}	97	0.964	3.0	8 – 69
	Mg^{2+}	97	0.948	1.9	4 – 38
	K^+	96	0.363	0.9	1 – 7
South Delta	**TDS**	231	0.997	11.3	73 – 906
	Br^-	256	0.887	0.06	0.03 – 0.78
	Cl^-	270	0.951	11.7	11 – 255
	SO_4^{2-}	231	0.921	15.3	9 – 254
	Alkalinity	231	0.915	9.3	27 – 173
	Na^+	270	0.984	4.9	9 – 179
	Ca^{2+}	270	0.908	4.7	8 – 76
	Mg^{2+}	270	0.962	1.6	3 – 42
	K^+	229	0.624	0.7	1 – 7.2

$R^2 > 0.90$ for all constituents except Br^- ($R^2 = 0.89$) and K^+ ($R^2 = 0.62$).

Location-Specific Urban Diversions

Special provisions were made to estimate TDS and ion concentrations at several urban diversions within the study domain, given unique needs related to meeting water-quality regulations and beneficial-use targets. Most, but not all, of these urban diversions are in the Old and Middle River export corridor sub-region of the interior Delta (see Appendix A). For some locations, we developed unique regression relationships. For other diversions, depending on their locations, we used boundary relationships in concert with the decision matrix to estimate TDS and ion concentrations from EC data. Location-specific regression constants and fitting statistics associated with the urban diversions at Barker Slough and Jones Pumping Plant are provided in Appendix B.

DISCUSSION

While continuous measurements of EC using electronic probes are abundant across the estuary, data on specific ion concentrations are more limited because such measurements generally require laboratory analysis. Ion-specific electrodes are commercially available for a limited number of ions; however, adoption of the technology is limited in the study area. This data gap belies the fact that information on ion-specific concentrations is important for managing water operations and municipal and agricultural source-water quality. The work presented here addressed this information need by developing a simple set of empirical relationships between EC, TDS, and eight major ionic constituents across the waters of the study area. Relationships between these constituents vary across space and time, and we performed an extensive data evaluation and grouping exercise—informed by a conceptual model of complex source-water mixing in the Delta over different seasons and water year types—to propose a set of model constants to quantify these relationships. Our analysis methodology built on previous work (Guivetchi 1986; Denton 2015) through use of a more complete data set and through proposing an expanded set of empirical equations that considered a broader range of locations and mixing conditions across the study area.

The basic goal of this work was to identify subsets of ionic data, for a particular region and/or season and hydrology, that were well explained when plotted together with EC or TDS as the controlling variable. The overall approach involved developing empirical relationships for the

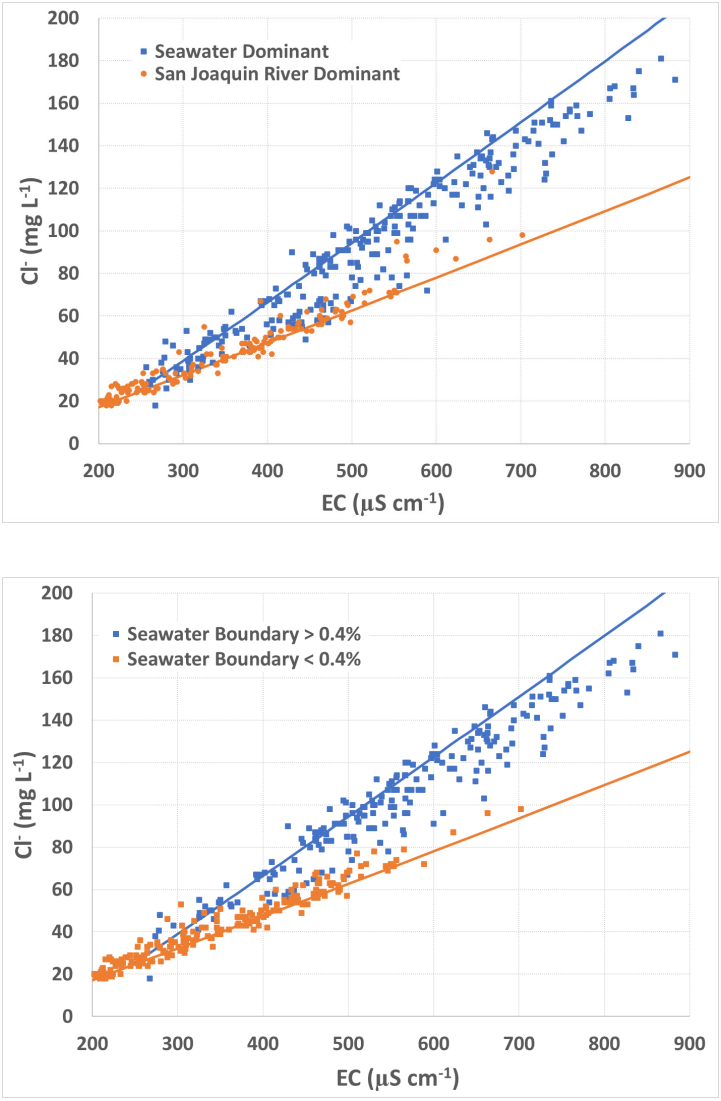

Figure 5 Observed relationship between Cl^- and EC at Banks Pumping Plant. The observed data are generally bounded by the San Joaquin River and the seawater boundary relationships (shown as *orange* and *blue lines*, respectively). Data in the top panel are sorted by in accordance with Table 1; data in the bottom panel are sorted following Hutton (2006, unreferenced, see "Notes"). Both sorting techniques give similar results.

boundary flows (that were largely independent of season) and identifying appropriate applications of these boundary relationships in the interior Delta, depending on proxy measures of prevailing hydrodynamic conditions (i.e., month, water year type, and X2 position). The interior Delta was divided into three sub-regions to account for the different hydrodynamic effect on source mixing in these sub-regions. This final step sought to find a parsimonious set of data groupings in the interior Delta where the relationships between EC, TDS and ionic concentrations could be represented with the least amount of noise. We developed additional equations for selected urban water-diversion locations, where we found the existing boundary equations to be inadequate. We linked the structured sets of equations developed through this empirical analysis to a decision tree to identify the most appropriate set to be used for a given location, season, and X2 position (when available).

Time-series trends in the boundary relationships between ionic concentrations and EC were not observed. We did not conduct formal trend analyses, because we have no basis for hypothesizing that such trends may exist over the available period of record. As noted in the Methods section, an exception relates to a step-change in the ionic make-up of pre-1982 San Joaquin River boundary data (not used in our work), a change driven by the accretion of saline water from gas wells along the Tuolumne River upstream of Vernalis (SDWA 1980; Kratzer and Grober 1991; Denton 2015) that were later capped. Similarly, we did not observe such time-series trends in the interior Delta, nor did we conduct formal trend analyses. However, unlike the boundary regions, we hypothesize that relationships with season, water year type, and X2 have in fact changed over time, but that such relationships have been relatively stationary since the 1970s, after construction of major upstream reservoirs and Delta export facilities as well as implementation of environmental regulations. Therefore, we recommend that the approach presented here for the interior Delta be used with caution when applied to conditions that pre-date the 1970s.

Although the data-grouping process in this work benefited from our conceptual understanding of how water flows through the study area—particularly the mixing of different source waters in the interior Delta—it is nonetheless an empirical exercise and not a substitute for

https://doi.org/10.15447/sfews.2023v21iss4art6

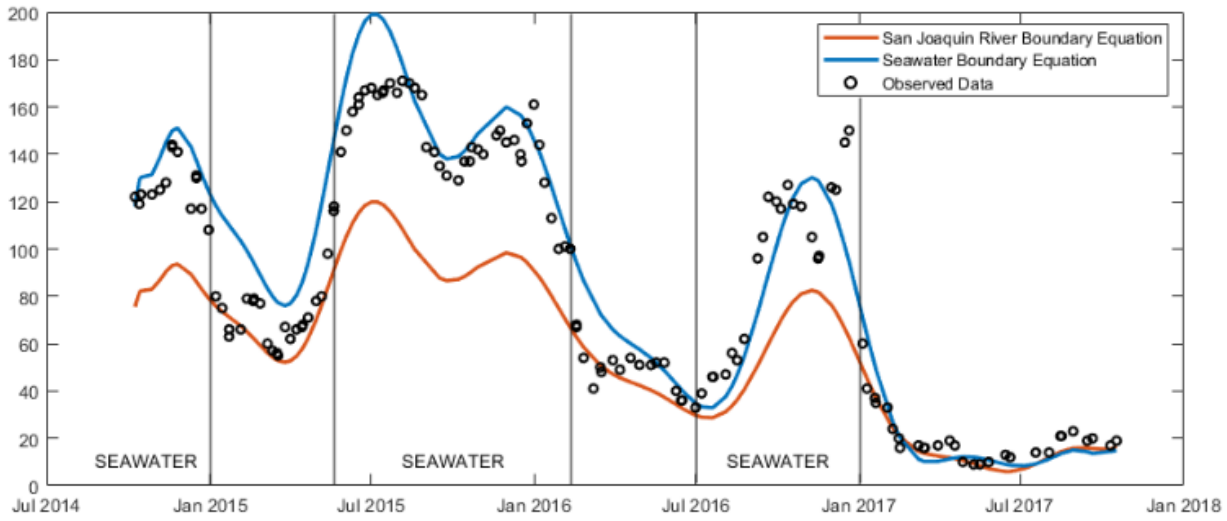

Figure 6 Three-year time series (October 2014 – September 2017) at Banks Pumping Plant comparing Cl^- grab sample data with EC-based predictions assuming San Joaquin River and seawater boundary relationships. The chart delineates periods of seawater dominance and San Joaquin River dominance (*unlabeled areas*) as predicted by Table 1 for the Old-Middle River export corridor sub-region. Water year 2015 is classified as "critical," 2016 is classified as "below normal," and 2017 is classified as "wet."

mechanistically based hydrodynamic and water-quality modeling. Such modeling frameworks exist for the study area (e.g., CDWR 2022) and, depending on study objectives, may be needed to obtain a more refined understanding of constituent relationships for specific hydrologic conditions and to explain variability at different temporal scales.

Some key limitations of the proposed simplified approach have been noted. One limitation is that the geographic boundaries for the different regions—seawater, freshwater, and San Joaquin River boundary regions and the interior Delta and sub-regions thereof—were not precisely defined but rather were developed accounting for similarities and differences in concentration ranges exhibited by the suite of grab-sample data compiled for this work. To avoid conflicting boundaries, and therefore conflicting methods of estimating constituent concentrations, the boundary regions were defined intuitively and are nominally bounded by major rivers, tributaries, and landmarks. The applicability of the proposed approach to locations not explicitly measured by the network of stations that were consulted (especially at or near regional interfaces) is worthy of further inspection. Within the interior Delta region, three sub-regions were defined based on locations of water-management facilities and an understanding that these and local inputs influence the observed hydrodynamic patterns. Agricultural drainage is a prevalent and important local input, and an analysis of its influence on salinity constituent relationships could potentially improve the confidence of estimates made within the interior Delta.

Another key limitation associated with the proposed approach is that, in the Old and Middle River export corridor sub-region of the interior Delta, the decision tree prescribes either the seawater or the San Joaquin River boundary as the dominant source water. However, some undiagnosed sources of scatter in the grab-sample data associated with this sub-region suggest that constituent concentrations may sometimes be systematically under- or over-estimated when the seawater boundary is prescribed and when EC is relatively high. For example, when EC exceeded 750 µS cm^{-1}, observed Br^- and Cl^- concentrations were sometimes lower than estimates computed using the seawater boundary relationships, while observed SO_4^{2-}, alkalinity, and Ca^{2+} concentrations were sometimes greater than the estimates. These concurrent over- and

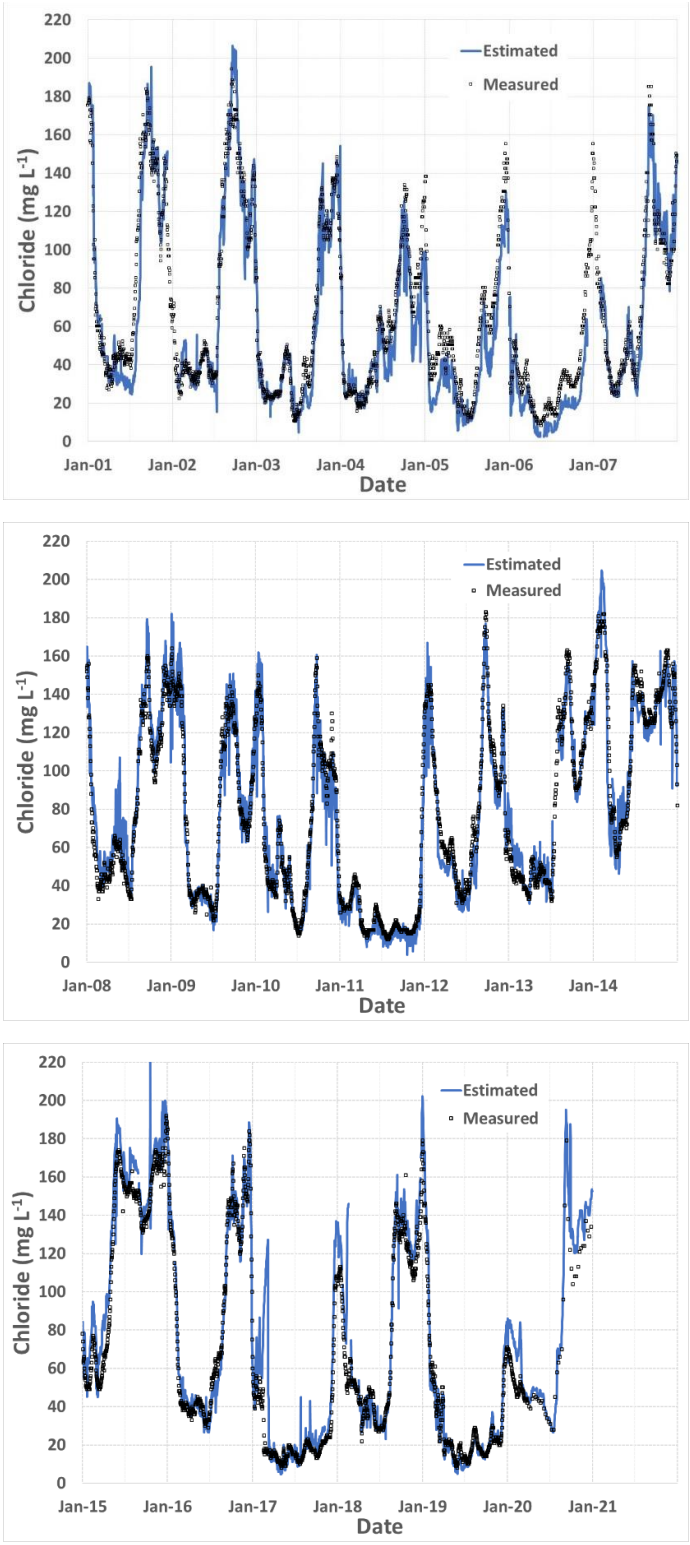

Figure 7 20-year time series (January 2001 – December 2020) at Old River @ Highway 4 (Contra Costa Water District Intake) comparing Cl^- grab sample data with EC-based predictions assuming San Joaquin River and seawater boundary relationships

under-estimations of constituent concentrations suggest that some local discharges with different ionic ratios than the San Joaquin River boundary would be a more appropriate dominant source water in these instances. It is also helpful to acknowledge that some agricultural discharges have been relocated in recent years (Denton 2005). These limitations point to areas in the interior Delta where more refined mechanistic or empirical analyses may be needed, particularly when additional source-water-quality data, such as for agricultural drainage, are reported. Where such data are available, application of machine learning techniques to inform prediction of complex EC-ion relationships in the interior Delta may prove useful (Namadi et al. 2022).

Despite the limitations discussed above and given ongoing water-user needs to obtain estimates of ionic concentrations, reliance on mechanistic model simulations is not always practical because the necessary skill sets, data inputs, and other project resources may not be available. For such situations, the availability of an empirical framework that can be readily deployed within a spreadsheet or even a database application provides estimates that can inform near-real-time decisions on water use and treatment. Toward this end, the results of this work are summarized in the form of a compact user guide, including the decision-tree described above that can be used to develop rapid estimates of ionic concentrations (or TDS) given EC or TDS measurements (Hutton et al. 2022b). Although future improvements are possible, as noted here, the decision tree and user guide tables capture patterns from more than 50 years of water-quality grab-sample data in the estuary and are expected to provide first-

https://doi.org/10.15447/sfews.2023v21iss4art6

order estimates of ionic concentrations to a broad stakeholder community.

ACKNOWLEDGEMENTS

Funding for this work was provided by the State Water Contractors MWQI Specific Projects Committee.

REFERENCES

[CDPW] California Department of Public Works. 1931. Variation and control of salinity in Sacramento–San Joaquin Delta and upper San Francisco Bay. Bulletin 27. [accessed 2023 Dec 06]. Available from: *https://www.waterboards.ca.gov/waterrights/water_issues/programs/bay_delta/deltaflow/docs/exhibits/ccwd/spprt_docs/ccwd_dpw_1931.pdf*

[CDWR] California Department of Water Resources. 2005. Water supply contract between the state of California Department of Water Resources and The Metropolitan Water District of Southern California for a water supply and selected related agreements. October 24. [accessed 2023 Dec 06]. Available from: *https://calisphere.org/item/ark:/86086/n22f7mgf/*

[CDWR] California Department of Water Resources. 2022. DSM2: Delta Simulation Model II. [accessed 2023 Dec 06]. Available from: *https://water.ca.gov/Library/Modeling-and-Analysis/Bay-Delta-Region-models-and-tools/Delta-Simulation-Model-II*

Cheng RT, Casulli V, Gartner JW. 1993. Tidal, Residual, Intertidal Mudflat (TRIM) model and its application to San Francisco Bay, California. Estuary Coast Shelf Sci. [accessed 2023 Dec 06];36(3):235–280. *https://doi.org/10.1006/ecss.1993.1016*

[CSWRCB] California State Water Resources Control Board. 1971. Delta Water Rights Decision 1379, July. [accessed 2023 Dec 06]. Available from: *https://www.waterboards.ca.gov/waterrights/board_decisions/adopted_orders/decisions/d1350_d1399/wrd1379.pdf*

[CSWRCB] California State Water Resources Control Board. 2000. Revised Water Right Decision 1641, March. [accessed 2023 Dec 06]. Available from: *https://www.waterboards.ca.gov/waterrights/board_decisions/adopted_orders/decisions/d1600_d1649/wrd1641_1999dec29.pdf*

Culkin F, Smed J. 1979. The history of standard seawater. Oceanol Acta. [accessed 2023 Dec 06];2(3):355–364. Available from: *https://archimer.ifremer.fr/doc/00122/23351/21178.pdf*

Denton RA. 1993. Predicting water quality at municipal water intakes–Part 1: Application to the Contra Costa Canal Intake. In: Shen HW, editor. Proceedings of the 1993 Hydraulic Division National Conference of the American Society of Civil Engineers. July 25-30, 1993; San Francisco. p. 809–814.

Denton RA. 2005. Letter to State Water Resources Control Board on Rock Slough compliance location (Issue 4b). February 14. [accessed 2023 Dec 06]. Available from: *https://www.waterboards.ca.gov/waterrights/water_issues/programs/bay_delta/wq_control_plans/2006wqcp/exhibits/append2/ccwd/ccwd-14.pdf*

Denton RA. 2015. Delta salinity constituent analysis, report prepared for the State Water Project Contractors Authority, February. [accessed 2023 Dec 06]. Available from: *https://rtdf.info/public_docs/Miscellaneous%20RTDF%20Web%20Page%20Information/Other%20MWQP%20and%20DWR%20Publications/Delta%20Salinity%20Constituents%20Report.pdf*

[DSC] Delta Stewardship Council. The Delta Plan. 2013. [accessed 2023 Dec 06]. Available from: *https://deltacouncil.ca.gov/delta-plan/.*

[Fed Regist] Federal Register. 1998. National primary drinking water regulations: disinfectants and disinfection byproducts. [accessed 2023 Dec 09];63(241). Available from: *https://www.govinfo.gov/content/pkg/FR-1998-12-16/pdf/98-32887.pdf*

Guivetchi K. 1986. Salinity unit conversion equations. California Department of Water Resources interoffice memorandum. accessed 2023 Dec 06]. Available from: *https://www.waterboards.ca.gov/waterrights/water_issues/programs/bay_delta/california_waterfix/exhibits/docs/petitioners_exhibit/dwr/dwr_316.pdf*

Hem JD. 1985. Study and interpretation of the chemical characteristics of natural water. USGS Water Supply Paper 2254. 3rd ed. Alexandra (VA): US Government Printing Office. Available from: *https://pubs.usgs.gov/wsp/wsp2254/pdf/wsp2254a.pdf*

Hutton PH, Chen L, Rath JS, Roy SB. 2019. Tidally-averaged flows in the interior Sacramento–San Joaquin River Delta: trends and change attribution. Hydrol Process. [accessed 2023 Dec 06]; 33(2):230–243. *https://doi.org/10.1002/hyp.13320*

Hutton PH, Chung FI. 1992. Simulating THM formation potential in Sacramento Delta: Part I. J Water Resour Plan Manag–ASCE [accessed 2023 Dec 06];118(5). *https://doi.org/10.1061/(ASCE)0733-9496(1992)118:5(513)*

Hutton PH, Rath J, Chen L, Ungs ML, Roy SB. 2016. Nine decades of salinity observations in the San Francisco Bay and Delta: modeling and trend evaluation. J Water Res Planning Manage. [accessed 2023 Dec 06];142(3). *http://doi.org/10.1061/(ASCE)WR.1943-5452.0000617*

Hutton PH, Rath JS, Roy SB. 2017a. Freshwater flow to the San Francisco Bay–Delta Estuary over nine decades. Part 1: trend evaluation. Hydrol Process. [accessed 2023 Dec 06];31(14):2500–2515. Available from: *http://onlinelibrary.wiley.com/doi/10.1002/hyp.11201/full*

Hutton PH, Rath JS, Roy SB. 2017b. Freshwater flow to the San Francisco Bay–Delta Estuary over nine decades. Part 2: change attribution. Hydrol Process. [accessed 2023 Dec 06];31(14):2516–2515. *https://doi.org/10.1002/hyp.11195*

Hutton PH, Roy SB. 2023a. Application of the practical salinity scale to the waters of San Francisco Estuary. Estuar Coast Shelf Sci. [accessed 2023 Dec 06];290:108380. *https://doi.org/10.1016/j.ecss.2023.108380*

Hutton PH, Roy SB. 2023b. Extension of the practical salinity scale to estimate major ion concentrations: application to the San Francisco Estuary. Estuaries Coasts. [accessed 2023 Dec 09];46:1375–1386. *https://doi.org/10.1007/s12237-023-01211-z*

Hutton PH, Roy SB, Krasner SW, Palencia L. 2022a. The Municipal Water Quality Investigations Program: a retrospective overview of the program's first three decades. Water. [accessed 2023 Dec 06];14:3426. *https://doi.org/10.3390/w14213426*

Hutton PH, Sinha A, Roy SB. 2022b. Simplified approach for estimating salinity constituent concentrations in the San Francisco Estuary and Sacramento–San Joaquin River Delta: a user guide. Report prepared for the State Water Contractors, July. [accessed 2023 Dec 06]. Available from: *https://rtdf.info/public_docs/Miscellaneous%20RTDF%20Web%20Page%20Information/Other%20MWQP%20and%20DWR%20Publications/2022-07-21%20MWQI%20Conservative%20Constituents%20User%20Guide_formatted.pdf*

Kimmerer W, Wilkerson F, Downing B, Dugdale R, Gross ES, Kayfetz K, Khanna S, Parker AE, Thompson J. 2019. Effects of drought and the emergency drought barrier on the ecosystem of the California Delta. San Franc Estuary Watershed Sci.[accessed 2023 Dec 06];17(3). *https://doi.org/10.15447/sfews.2019v17iss3art2*

Kratzer C, Grober L. 1991. San Joaquin River salinity: 1991 projections compared to 1977. Calif Agric. [accessed 2023 Dec 06];45(6):24–27. Available from: *https://calag.ucanr.edu/Archive/?article=ca.v045n06p24*

Lewis EL. 1980. The practical salinity scale 1978 and its antecedents. IEEE J Oceanic Engineer. [accessed 2023 Dec 06];5(1):3–8. *http://doi.org/10.1109/JOE.1980.1145448*

Lund JR, Hanak E, Fleenor WE, Bennett WA, Howitt RE, Mount JF, Moyle PB. 2010. Comparing futures for the Sacramento–San Joaquin Delta. Berkeley (CA): University of California Press. 231 p.

[IEP et al.] Interagency Ecological Program, Martinez M, Perry S. 2021. Interagency Ecological Program: discrete water quality monitoring in the Sacramento–San Joaquin Bay-Delta, collected by the Environmental Monitoring Program, 1975-2020. ver 4. accessed Oct 24 2023]. Environmental Data Initiative. *https://doi.org/10.6073/pasta/31f724011cae3d51b2c31c6d144b60b0*

Millero FJ, Feistel R, Wright DG, McDougall TJ. 2008. The composition of standard seawater and the definition of the reference-composition salinity scale. Deep-Sea Res (Part 1: Deep Oceanic and Research Papers). [accessed 2023 Dec 06];55(1): 50–72. *https://doi.org/10.1016/j.dsr.2007.10.001*

Monsen NE, Cloern JE, Burau JR. 2007. Effects of flow diversions on water and habitat quality: examples from California's highly manipulated Sacramento–San Joaquin Delta. San Franc Estuary Watershed Sci. [accessed 2023 Dec 06];5(3). *https://doi.org/10.15447/sfews.2007v5iss5art2*

Montoya BL. 2007. Sources of salinity in the south Sacramento–San Joaquin Delta. CDWR office memorandum, May 30. 46 p.

Najjar RG, Herrmann M, Cintrón Del Valle SM, Friedman JR, Friedrichs MAM, Harris LA, Shadwick EH, Stets EG, Woodland RJ. 2019. Alkalinity in tidal tributaries of the Chesapeake Bay. J Geophys Res–Oceans. [accessed 2023 Dec 06];125:e2019JC015597. *https://doi.org/10.1029/2019JC015597*

Najm IN, Krasner SW. 1995. Effects of bromide and NOM on by-product formation. J Am Water Works Assoc. [accessed 2023 Dec 06];87(1):106–115. *https://doi.org/10.1002/j.1551-8833.1995.tb06305.x*

Namadi P, He M, Sandhu P. 2022. Salinity-constituent conversion in South Sacramento–San Joaquin Delta of California via machine learning. Earth Sci Inform. [accessed 2023 Dec 06];15:1749–1764. *https://doi.org/10.1007/s12145-022-00828-1*

Pawlowicz R. 2010. A model for predicting changes in the electrical conductivity, practical salinity, and absolute salinity of seawater due to variations in relative chemical composition. Ocean Sci. [accessed 2023 Dec 06];6:361–378. Available from: *www.ocean-sci.net/6/361/2010/*

Roy SB, Hutton PH, Heidel K, Rath J, Sinha A. 2021. Protocols for water and environmental modeling. California Water and Environmental Modeling Forum, November 19. [accessed 2023 Dec 06]. Available from: *https://cwemf.org/wp/resources-3/modeling-protocols-report/*

Schemel L. 2001. Simplified conversions between specific conductance and salinity units for use with data from monitoring stations. Interagency Ecological Program Newsletter. [accessed 2023 Dec 06];14(1). *https://pubs.usgs.gov/publication/70174311*

[SDWA] South Delta Water Agency. 1980. Effects of the CVP upon the southern Delta Water Supply—Sacramento–San Joaquin River Delta, California. Report prepared jointly with the Water and Power Resources Service, June. 179 p.

Van Winkel W, Eaton FM. 1910. The quality of the surface waters of California. USGS Water Supply Paper 237. [accessed 2023 Dec 06]. Available from: *https://pubs.usgs.gov/publication/wsp237*

Wagner ED, Plewa MJ. 2017. CHO cell cytotoxicity and genotoxicity analyses of disinfection by-products: an updated review. J Environ Sci. [accessed 2023 Dec 06];58:64–76.

Wallace WJ. 1974. The development of the chlorinity/salinity concept in oceanography. Elsevier Oceanography Series 7. [accessed 2023 Dec 06]. Amsterdam (The Netherlands): Elsevier. 227 p.

Wright DG, Pawlowicz R, McDougall TJ, Feistel R, Marion GM. 2011. Absolute Salinity, "Density Salinity" and the Reference-Composition Salinity Scale: present and future use in the seawater standard TEOS-10. Ocean Sci. [accessed 2023 Dec 06];7:1–26. *https//:doi.org.doi:10.5194/os-7-1-2011*

NOTES

Hutton PH. 2006. Validation of DSM2 volumetric fingerprints using grab sample mineral data. Presented at the California and Environmental Modeling Forum Annual Meeting. 2006 Feb 28–Mar 2; Pacific Grove. Available from: *https://www.cwemf.org/Asilomar/PaulHuttonPresentation.pdf*